Atmospheric Soundings in Near-Real Time from Combined Satellite and Ground-Based Remotely Sensed Data

JAMES COGAN AND EDWARD MEASURE

U.S. Army Research Laboratory, White Sands Missile Range, New Mexico

DANIEL WOLFE

Environmental Technology Laboratory, National Oceanic and Atmospheric Administration, Boulder, Colorado

(Manuscript received 8 July 1996, in final form 10 March 1997)

ABSTRACT

A mobile profiling system has been developed that is capable of probing the atmosphere from the surface to over 30 km. The Mobile Profiling System (MPS) combines ground-based instruments, including a five-beam 924-MHz radar wind profiler, a radio acoustic sounding system, and two passive microwave sounders, with a receiver and processor for meteorological satellite data. Software in the MPS produces profiles from the surface to the highest satellite sounding level by combining surface data and profiles generated from the suite of ground-based sensors with those from a meteorological satellite. The algorithms generate soundings of temperature, humidity, wind velocity, and other meteorological variables. The method for combining data from the separate sources is not site specific and requires no a priori information. The MPS has the potential for a variety of applications, including detailed analysis of meteorological variables for research and operations over mesoscale areas, such as regional pollution studies and severe storm forecasting. This paper describes the method for merging data from satellite and ground-based remote sensing systems, and presents results from a series of field tests of both individual sensors and combined soundings. Accuracy of the combined soundings appears comparable to that from rawinsonde with the exception of wind velocity at satellite sounding altitudes. The MPS has operated successfully in several different climates: in the Los Angeles Free Radical Experiment at Claremont, California, and in tests at White Sands Missile Range, New Mexico; Erie, Colorado; Ft. Sill, Oklahoma; and Wallops Island, Virginia.

1. Introduction

Ground-based systems currently in use for operational measurement of atmospheric profiles rely heavily on balloonborne rawinsondes. The time between balloon launches may be as little as 1–4 h during field experiments but, in normal operations, launches occur every 12 h. The National Oceanic and Atmospheric Administration's (NOAA) National Profiler Network (NPN), consisting of 404-MHz radars at fixed sites mostly in the central United States, can provide wind profiles every hour (Barth et al. 1994; Ralph et al. 1995; Weber et al. 1990; Strauch et al. 1984). Some sites also are equipped with radio acoustic sounding systems (RASS), providing profiles of virtual temperature T_v. Meteorological satellite sounders using either infrared or microwave (MW) wavelengths provide a means of obtaining atmospheric soundings on a routine basis for

regions where surface and upper-air stations are absent. However, for mesoscale areas over land, satellite sounder data may have horizontal and vertical resolutions that are too coarse for certain applications, especially for the lower troposphere. Orlanski (1975) defines various mesoscale size ranges.

In the lowest 1 or 2 km over land, satellite temperature T soundings without ancillary data generally have errors of as much as 5–8 K (Jedlovec 1985; Le Marshall 1988; Reale 1990). For derived variables such as wind velocity, the situation may be even less desirable (Franklin and Lord 1988). Vertical and horizontal resolutions typically are about 3–5 km and around 30–200 km, respectively, depending on whether infrared or MW sounders are used and the amount of spatial averaging for noise reduction (Heacock 1985; Shenk et al. 1987; Swadley and Chandler 1992).

The Mobile Profiler System (MPS) (Wolfe et al. 1995) being developed by the Army Research Laboratory (ARL) and NOAA's Environmental Technology Laboratory (ETL) can provide soundings in the troposphere as often as once every 3 min. The radar wind profiler operating at 924 MHz can provide wind profiles with a vertical resolution of 100 m up to a height of 3–5 km

Corresponding author address: Dr. James Cogan, U.S. Army Research Laboratory, AMSRL-IS-EA, Bldg. 1622, White Sands Missile Range, NM 88002-5501.
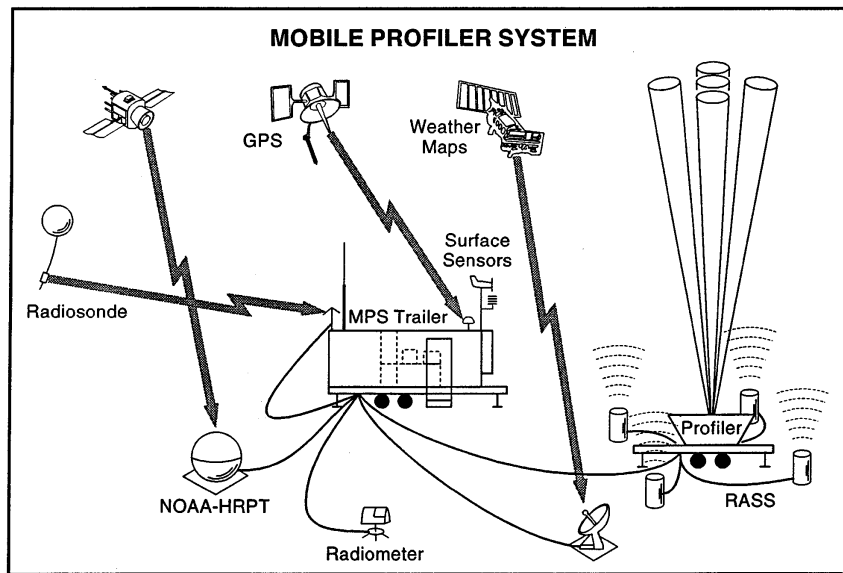E-mail: jcogan@arl.mil

FIG. 1. Layout of primary systems in the mobile profiling system (MPS) from Wolfe et al. (1995).

on average, depending on atmospheric conditions. Under certain atmospheric conditions (i.e., moist and turbulent) heights over 6 km are possible. The RASS can produce soundings of T_v up to around 0.8–1.6 km, again depending on atmospheric conditions, at a vertical resolution of about 100 m. A microwave radiometer operating in the oxygen band from 50–60 GHz is able to produce useful T, or T_v, profiles to an altitude of around 3–5 km. A second radiometer produces estimates of total water content (vapor and liquid). A new radiometer currently under evaluation will replace both older radiometers in a package smaller than either are now. The MPS receives direct readout data from the NOAA series of polar-orbiting satellites. The satellite receiver and processor system is being upgraded to a smaller but more capable version that will have the additional capability to obtain direct readout data from Defense Meteorological Satellite Program (DMSP) satellites. The MPS has certain elements in common with fixed-site systems described by Parsons et al. (1994) and Stokes and Schwartz (1994) but has a number of additional features. These additions include software for processing and quality control of data from the ground-based sensors and for combining satellite soundings with ground-based profiles in near-real time. Wolfe et al. (1995) provide details on the MPS as configured and operated during the Los Angeles Free Radical Experiment (LAFRE) in Claremont, California, and present examples of the various data processing and output available. Cogan (1995) presents additional samples of output and gives preliminary quantitative results. Figure 1, from Wolfe et al. (1995), shows the primary sensors in the MPS as configured during the LAFRE. Table 1 presents certain instrument characteristics and compares the earlier configuration as in the LAFRE with that incorporating recent and ongoing changes.

The merging method for combining ground-based and satellite profiles described in this paper is a revised version of the technique described in Cogan and Izaguirre

TABLE 1. MPS sensors and characteristics. Initial configuration compared with that from recent and ongoing upgrades. New version has a smaller, more robust shelter for processors and some instruments.

System	Initial MPS as during LAFRE	MPS with new/ongoing upgrades
Radar wind profiler	924 MHz, phased array	Combined phased array wind radar (924 MHz) and RASS (~2000 Hz), 120 transducers in RASS
RASS	~2000 Hz, 4 external sources	
MW radiometer	T: 50–60 GHz (O_2), PW, LW: 20.7, 31.4 GHz, 2 radiometers (T, PW/LW)	One radiometer operating in same frequency bands for same variables, smaller than either of older radiometers
Satellite receiver and processor	HRPT from NOAA satellites (soundings and imagery)	Upgraded, smaller system: HRPT from NOAA and direct readout DMSP
Portable surface station	Standard meteorological variables—mast mounted on trailer	No change
Weather map receiver	Receive maps and other data via GOES	Eliminated GOES link, maps, and other weather data via Internet
GPS receiver	Provides site location	No change

TABLE 2. Capabilities of several remote sensing and rawinsonde systems. The values shown represent averages for most current systems in each group.

System	Variable	Capabilities			
		Accuracy	Temporal resolution	Vertical resolution	Vertical range
Radar profiler 915/924 MHz	Wind speed	±1.5 to 3 m s^{-1}	3–6 min (Consensus methods may need up to 30 min)	100 m	100–5000 m
	Wind direction	$\pm10°$ to 15°			
RASS	Virtual temp	±1 to 2 K			100–1600 m
Microwave radiometer	Temperature or virtual temp	±1 to 3 K	3 min	Variable	Up to 10 km
Satellite sounder (TOVS, SSM/T-1)	Temperature	±2 to 2.5 K	5 h (2 Sat) 4 h (3 Sat) (1–2 h near poles)	3–5 km	2–40 km
	Wind speed	±4 to 14 m s^{-1}			
	Wind direction	$\pm10°$ to >30°			
Rawinsonde	Temperature	±0.5 to 1 K	1–2 h depending on max. height	Point value 60–600-m layers	Surface–30 km
	Wind speed	±0.5 to 2 m s^{-1}			
	Wind direction	$\pm5°$ to 10°			

(1993). This method may be used for T_v, pressure, wind velocity, and other meteorological variables. Even though the MW radiometer component of the MPS uses a statistical method for retrieval of temperature profiles and moisture parameters that needs a priori data, the merging algorithm itself may be applied wherever the MPS is located; that is, it is not site specific and requires no a priori information. However, the user may alter certain software parameters (e.g., output layer thickness or maximum distance from the MPS site for acceptance of satellite profiles). Current statistical techniques for merging ground-based and satellite profiles of T (or T_v) reported in the literature (Westwater et al. 1984a; Westwater et al. 1984b; Schroeder et al. 1991) are site specific in that statistical coefficients are computed using a large set of a priori data normally gathered for a long series of rawinsonde soundings from a particular location.

Here we discuss the characteristics of instruments of the type employed in the MPS and describe the method for merging satellite and ground-based profiles into a combined sounding. We present results of field tests of both combined soundings and profiles from individual ground-based sensors. Comparisons with rawinsondes and radar-tracked pibals give an idea of how these systems compare with more traditional sounding systems.

2. Sensor characteristics

Before evaluating the merging algorithm and accuracies of the component sensors, the accuracies and other relevant measurement parameters of similar data sources from the formal literature should be examined. Of particular interest are the satellite sounders and ground-based radar profilers, RASS, and MW radiometers used in the MPS. Table 2 summarizes certain information extracted from Moran and Strauch (1994), Flowers et al. (1994), Okrasinski and Olsen (1991), Weber and Wuertz (1990), Weber et al. (1990), Reale (1990), May et al. (1989), Le Marshall (1988), Franklin and Lord (1988), and Jedlovec (1985). These values

may be compared with similar data for common rawinsonde systems (Fisher et al. 1987), also presented in Table 2.

From Table 2 we see that ground-based radar profilers and RASS have accuracies that approach those of some operational rawinsonde systems. Flowers et al. (1994) note that the RASS performance may be reduced under certain conditions (e.g., strong near-surface winds), and the extreme cases they reported are not included in the table. All the systems in Table 2 produce measurements of a volume or layer average, except rawinsonde values of T. A radar profiler obtains a mean wind over a volume, with a horizontal scale on the order of tens to thousands of meters depending on altitude from the radar, beam elevation angle, and beamwidth. For a system such as 404-, 449-, or 50-MHz radars, the volume represented by the three (or five) beams used to measure the horizontal and vertical wind may have a horizontal diameter exceeding 10 km near 15- or 20-km altitude. The radar processing algorithms developed by ETL for the MPS (Wolfe et al. 1995) represent an improvement over the standard consensus techniques. These algorithms allow for higher data quality at faster data rates than previously possible. Errors in wind measurements caused by migratory birds (Wilczak et al. 1995) have been addressed through a new spectral averaging method (Merritt 1995). Although limited when bird densities are high, this algorithm attempts to identify interference in the spectral data prior to averaging, thereby retaining more useful wind information.

Vertical profiles of T or T_v can be inferred from measurements of MW brightness temperatures. For surface-based measurements, in the 20–60-GHz region, the measured brightness temperatures approximately satisfy the following equation:

$$T_{bv} = \int_0^\infty T(z)\alpha_\nu(z) \exp\left[-\int_0^z \alpha_\nu(z')\,dz'\right]dz$$
$$+ T_{bv}^\infty \exp\left[-\int_0^z \alpha_\nu(z)\,dz\right], \tag{1}$$

where $T_{b\nu}$ is the downwelling MW brightness temperature at frequency ν; $T(z)$ is the temperature at height z; $\alpha_\nu(z)$ is the absorption coefficient; and $T_{b\nu}$ is the downwelling cosmic MW background brightness temperature above the atmosphere.

Inferring atmospheric temperature structure from MW brightness temperature measurements thus becomes the problem of solving (inverting) Eq. (1) to find $T(z)$. A database of past radiosonde observations has been used to calculate corresponding received radiances at our operating frequencies. Our temperature profiles are calculated with regression coefficients computed from the database radiances and corresponding radiosonde observations. The absorption coefficient $\alpha_\nu(z)$ in the frequency region of interest is due mainly to oxygen lines (50–60 GHz), the water vapor line at 22.235 GHz, and a liquid water continuum measured at 31.4 GHz. Oxygen is well mixed in the atmosphere so a good a priori estimate of its contribution is possible. In our scheme, water vapor and liquid water are independently measured by radiometric channels near 20.7 and 31.4 GHz. Vertical resolution is about 30 m at heights below 1 km, increasing to more than 1 km around 10 km.

Satellite sounders measure radiances that are converted to temperatures that represent means for large volumes of atmosphere, according to the frequency-dependent weighting functions and horizontal field of view. Temporal resolutions in Table 2 are average values. Generally, satellite values are valid for altitudes greater than 2 or 3 km above a land surface and not near the tropopause (e.g., temperature is ±5–8 K near the surface, and ±3–5 K near the tropopause). A temperature may represent the mean over a vertical extent of 3–5 km and over a horizontal area of tens to over 100-km diameter (assuming a circular area). Wind velocity is derived from the satellite T profile normally using geostrophic, gradient, or thermal wind equations (Franklin and Lord 1988). A rawinsonde acquires a mean-layer wind velocity along its path, over a period of perhaps 1 min or less (most rawinsondes rise at about 5 m s^{-1}); T measurements may be considered as point values. Temporal resolution of less than 1 h may be achieved for rawinsonde if there is a capability for multiple transmitter frequencies. Table 2 provides an indicator of the relative "quality" of data from the listed sensors inclusive of inherent differences between them due to measurement and processing methods. However, satellite sounders are the only means of obtaining large area or global coverage, while radar profilers with RASS and MW radiometers have the best spatial and temporal resolution.

3. Merging algorithms

The algorithms described here combine profiles from a suite of ground-based systems and satellite sounders. A radar profiler, RASS, and an MW radiometer provide data below the lowest satellite level. Currently, RASS

values of T_v are used up to the highest RASS data level. Above that height radiometer values are used, when available, up to the maximum height of "useful" data (nominally about 3.5 km based on early test results). The combined RASS and radiometer profile is the ground-based profile of T_v. Where ground-based and satellite profiles overlap, the satellite data are weighted in accordance with the spatial and temporal separation of the sounding from the ground-based profiles (here we will refer to the radar wind profiler RASS and radiometer combination as the profiler). The spatial weighting function has an elliptical form

$$W = 1 - \frac{X^2}{A^2} - \frac{Y^2}{B^2},\qquad(2)$$

where W is weight, A and B are the semimajor and semiminor axes of the assumed elliptical area represented by the satellite sounding (greater or equal to the horizontal resolution of a single satellite profile), and X and Y are the distances along those axes from the profiler to the center of the satellite sounding footprint. For polar-orbiting satellites a circular area may be sufficient away from the edges of the swath, say within 500 or 600 km of the subsatellite track. Some misregistration with height can occur as nadir angle increases, especially toward the edges of the swath. The temporal weighting function has an initial period when the two sources of data have equal weight (e.g., 15 min), followed by a period of linear decrease to some time (usually 3–6 h) when the satellite data are ignored (temporal weight equals 0). The final weight given to the satellite sounding is the product of the spatial and temporal weights times an accuracy ratio R. This ratio relates typical accuracies (Table 2) of the radar wind profiler RASS (T_v) and radiometer (T or T_v estimate) to those of the satellite sounder. For current instruments R decreases the weight given to the satellite data. The user may alter these parameters.

The satellite and ground-based profiles may overlap or a gap may occur between them. When the profiles overlap, the satellite data are interpolated to profiler heights in the overlap region. The equation for combining the two sets of data for those heights has the following form:

$$Q = W(Q_p + Q_s)/2 + (1 - W)Q_p,\qquad(3)$$

where Q is a variable at some height, W is here the combined temporal and spatial weight times the accuracy ratio R, and subscripts p and s refer to profiler and satellite, respectively.

Where the data do not overlap, a gap exists between the highest altitude of a ground-based profile and the lowest height of the satellite data. In this case the satellite data are extrapolated down to the maximum altitude of the ground-based profile. Above the highest altitude of the profiler data for either T_v or wind velocity, the satellite value is adjusted according to a scheme described in Cogan and Izaguirre (1993). It is based on
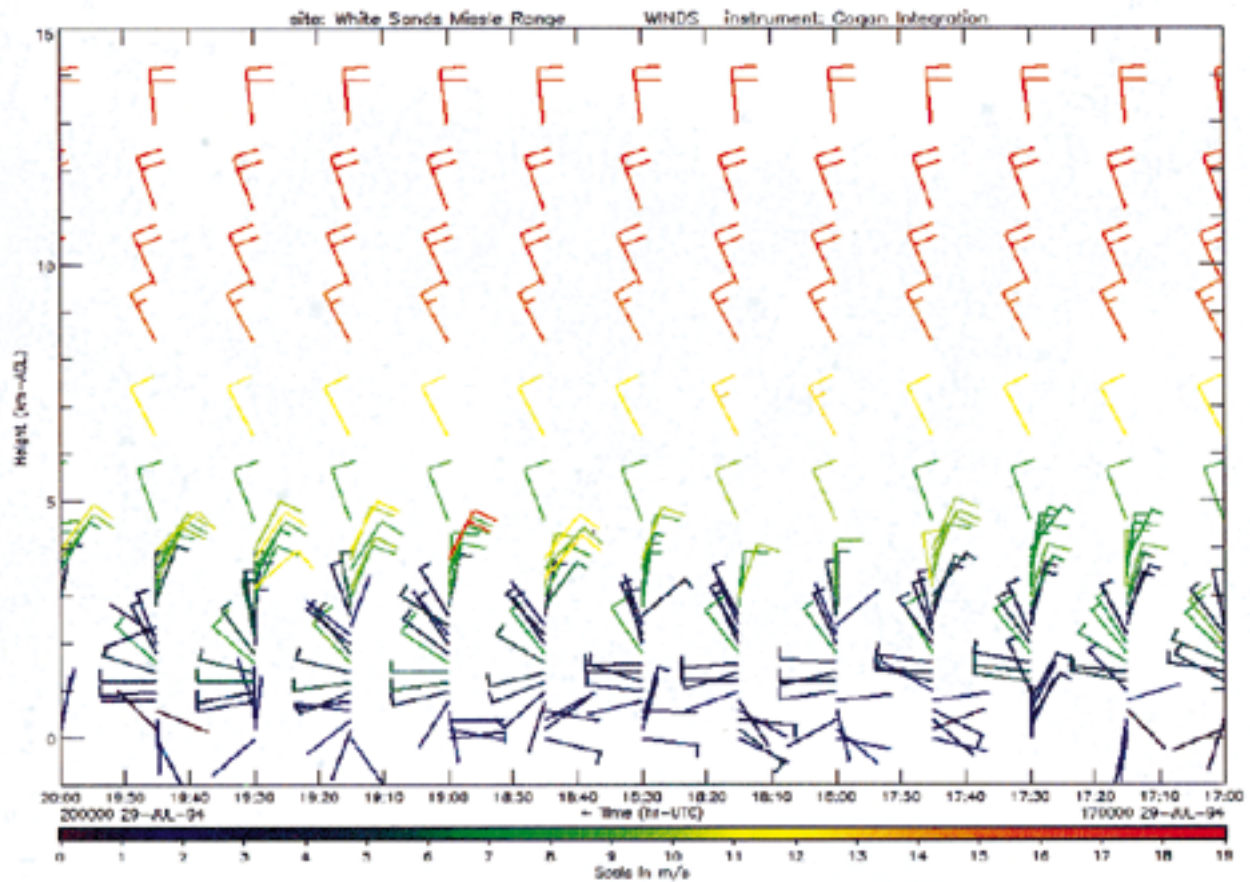
FIG. 2. Time–height wind barb plot for 29 July 1994 at WSMR, New Mexico, from Cogan (1995).

the difference between satellite (actual or extrapolated) and profiler values at the maximum profiler height for the particular variable. The adjustment or correction is reduced in magnitude through multiplication by an adjustment parameter α at successive heights up to a preset number of satellite levels (i.e., $D_i = \alpha[D_{i-1}]$, where D is the difference value and i is a satellite sounding level). Normally, data are adjusted for three to five satellite levels above the highest profiler level; α and the number of levels may be altered by the user. If the gap between the highest profiler level and the satellite level immediately above exceeds a preset value (e.g., 2 or 3 km) the algorithm skips the extrapolation routine and does not adjust the satellite data. Each satellite T profile is converted to T_v using retrieved dewpoints, if available; otherwise, the program uses a rough estimate based on the surface value of humidity. Alternatively, a profile based on, say, regional climatology could be used. At the heights of satellite data used here, greater or equal to 2.5 km above ground level (AGL), T_v often is within 1 K of T. No conversion takes place if T or dewpoint is less than 233 K, or $z \geq 10$ km.

Figure 2 shows plots of combined soundings of wind velocity for the period 1700–2000 UTC 29 July 1994

at White Sands Missile Range (WSMR), New Mexico. Each wind profile is a 15-min average ending at the time when the profile is plotted. Wind barbs plotted near 4.8, 6.4, and 8.3 km are satellite-derived geostrophic winds modified according to the aforementioned method.

4. Results and comparisons

a. Los Angeles Free Radical Experiment

Personnel from ARL and ETL participated in the Los Angeles Free Radical Experiment (LAFRE), using the MPS to obtain detailed sounding data for the primary sponsor—the California Air Resources Board. These data also served to check out the system and algorithms. The MPS operated almost continuously from 28 August 1993 through 23 September 1993. During this period a MARWIN and Cross-chain Loran Atmospheric Sounding System (CLASS) were operated simultaneously from the MPS trailer. The ability to operate rawinsondes from the MPS allowed for detailed intercomparisons. Near-real-time graphical and statistical comparisons were possible using software developed by ETL and
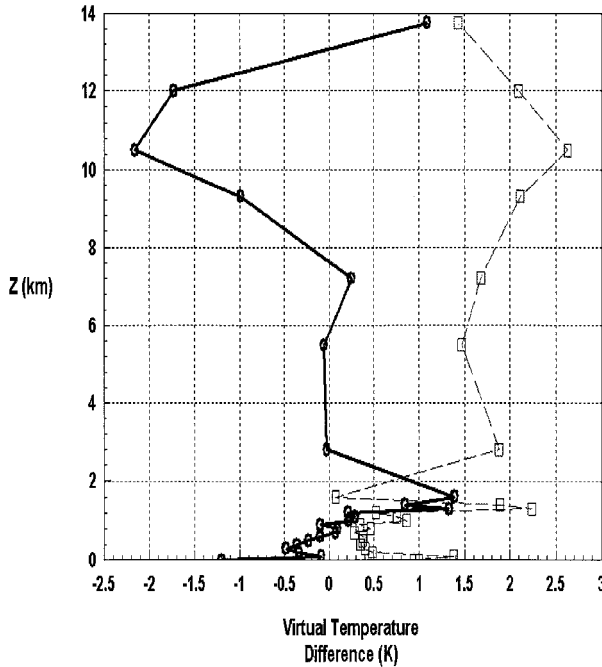
FIG. 3. Mean (solid line) and standard deviation (dashed line) of T_v(K) differences (MPS minus rawinsonde) for 7–11 September 1993. Heights are AGL.
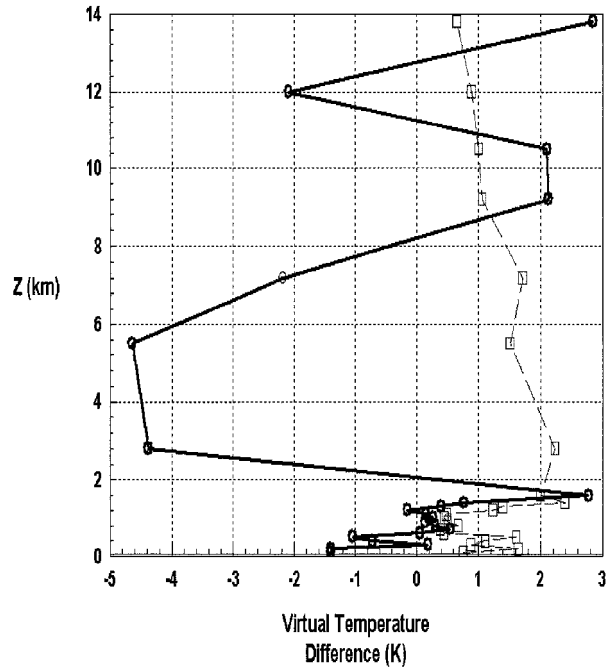

FIG. 4. Same as in Fig. 3 except for 17–23 September 1993.

ARL (Wolfe et al. 1995; Cogan 1995). The MW radiometer (temperature only) operated during only part of the LAFRE, and the merged profiles discussed here do not include MW data.

From 28 August through 11 September 1993 the Los Angeles basin was under a strong upper ridge and, at times, a closed high pressure area from the surface through 300 hPa. The marine boundary layer was consistently capped by one or more inversions. Wolfe et al. (1995) and Cogan (1995) present charts that show wind velocities from the radar profiler for typical days during this early part of the LAFRE, depicting light and often variable winds. Combining these profiles with the nearest good satellite sounding, sometimes as much as 300-km distant, led to a "worst-case" situation on several days. Atmospheric conditions, especially wind velocity, are often quite different 200 or 300 km to either side of a strong ridge.

Figures 3–6 show merged profiles from the LAFRE data compared with rawinsonde data for 0.1-km averaged layers. Figure 3 contains up to 36 potential comparisons during 7–11 September compared with a maximum of 12 during 17–23 September for Fig. 4. During the second period comparisons were obtained on 17 and 20–23 September. Figures 5 and 6 show the RASS values of Figs. 3 and 4, respectively, in an expanded scale for heights less than 2 km. For these comparisons RASS T_v were corrected for vertical velocity in a manner similar to that employed by Moran and Strauch (1994). These results suggest that the greatest differences may

occur within any layer of atmosphere and are not uniformly distributed with height.

Figure 3 shows a fairly typical pattern (e.g., accuracy degraded near the tropopause) of standard deviation σ_τ of T_v differences at satellite levels with values somewhat lower than previously published (Le Marshall 1988; Reale 1990). The merging of satellite and RASS profiles
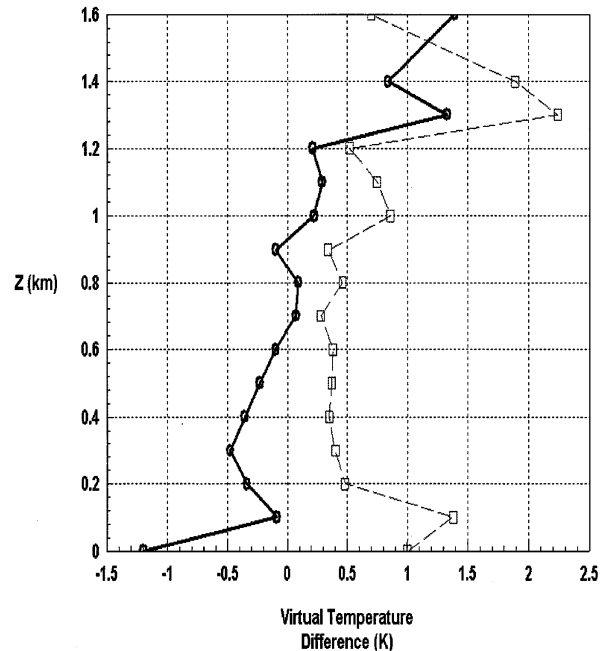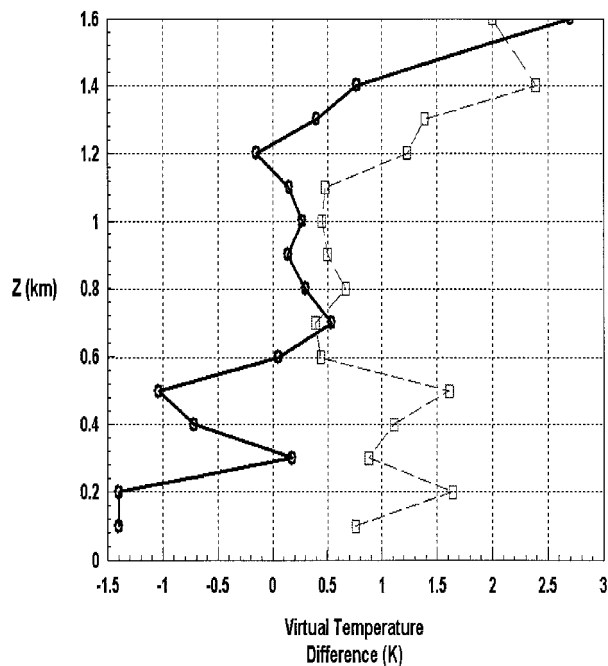

FIG. 5. Same as Fig. 3 but for RASS only.

FIG. 6. Same as in Fig. 4 but for RASS only.

greatly reduced the differences in the lowest few kilometers relative to satellite soundings alone (about 0.5–2 K vs 5–8 K). Figures 3 and 5 show that the magnitude of mean differences and σ_τ values for the RASS are fairly small (<0.5 and <0.9 K, respectively, for $0.1 < z < 1.3$ km), except at the highest RASS levels (≥ 1.3 km) and near the surface (≤ 0.1 km). Figure 4 presents a less common distribution of values with height z at satellite levels. The σ_τ of T_v differences decreases near the tropopause, and the mean of the differences is high at lower satellite levels in spite of a reduction in magnitude as a result of the merging process. In Figs. 4 and 6 the RASS values of σ_τ are higher at $z \leq 0.5$ km and at $z \geq 1.3$ km. Magnitude of the mean differences for RASS is high at some lower layers and at 1.6 km. These results are not unexpected. In the lower layers, surface heating and cooling cause greater variability. The higher layers, near the maximum range for RASS, often coincided with the height of the marine inversion. Variability in height and strength of this inversion and its relationship to location and thickness of combined sounding layers are significant factors when comparing with rawinsonde soundings.

The lower σ_τ near the tropopause during the second period may have arisen as a result of a weaker lapse rate, or little change in it, near the tropopause, and possibly as a result of a lower horizontal temperature gradient near the tropopause over the area in and around the Los Angeles basin during most or all of the second period. The former would tend to reduce inaccuracies in the satellite data due to the inherent smoothing of vertical temperature gradients and errors induced by incorrect height attributed to a satellite value. The latter would tend to lower temperature differences between satellite and rawinsonde that occur because of horizontal distance between satellite sounder field of view and rawinsonde location. An investigation of sounding data from three stations near the Los Angeles basin indicated that the magnitude of the lapse rate from about 11 to 14 km (below the tropopause) was about 1.2 K km^{-1} to about 1.7 K km^{-1} smaller during the comparison days of the second period (average) depending on the station. Also, the tropopause was about 2–3 K warmer during the second period. Upper-air maps for 200 hPa (12.1 km $< z <$ 12.5 km), near the top of the combined soundings from the LAFRE, showed a more zonal distribution of temperature during the second period than during the first. The mean and standard deviation of the magnitude of the horizontal lapse rate within 300 km of the test site showed almost no change for the east–west gradient. Small increases in magnitude of mean and standard deviation of about 0.1 to 0.2 K per 100 km each appeared for the north–south gradient from the first to second period. An increase in the north–south gradient would be expected as the distribution of temperature became more zonal. However, the smoothing of horizontal temperature gradients in satellite data (Jedlovec 1985) would tend to further reduce the effect, if noticeable, of those small changes. While the effect on temperature differences between satellite and rawinsonde would have been minimal from the changes in the horizontal gradient noted above (very small increase in σ_τ), the more significant decrease in vertical temperature gradient and the warmer tropopause during the second period (relatively large decrease in σ_τ) may at least partly explain the reduction in σ_τ in the few kilometers below the tropopause.

Table 3 shows means and standard deviations of wind speed differences in meters per second for the radar profiler and satellite (adjusted at the lowest three satellite data levels) relative to rawinsonde. The maximum

TABLE 3. Means and standard deviations of wind speed differences (m s^{-1}) for 0.3-km layers (indicated sensor minus rawinsonde) obtained during the LAFRE.

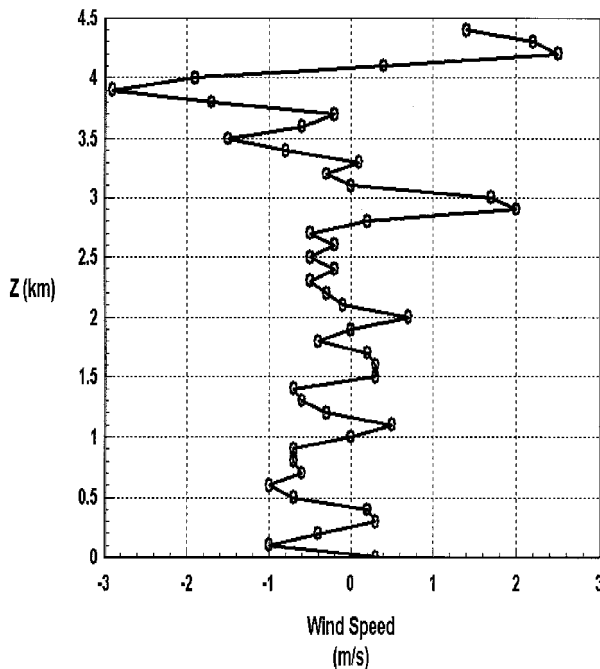| Mean		Standard deviation		Number of layers		Days (1993)	
Radar profiler	Satellite	Radar profiler	Satellite	Radar profiler	Satellite	Radar profiler	Satellite
0.75	10.84	1.88	8.60	14	6	7–11 Sep	
1.53	8.61	2.75	2.88	11	6	17, 20–23 Sep	

FIG. 7. Wind speed differences (m s^{-1}) between CLASS and MAR-WIN systems for one ascent from LAFRE data. Heights are AGL.

number of data comparisons by layer are the same as for the T_v comparisons presented above.

At times the rawinsonde data may contain serious errors. Fisher et al. (1987) present information on the average errors found in several types of rawinsonde systems. To gain an idea of the quality of the rawinsonde data from the LAFRE, soundings were compared with two similar systems (MARWIN and CLASS) receiving data from one sonde. Differences in T_v from comparisons using a single sonde averaged around ±0.2–0.4 K, with maximum differences of about ±1 K. Figure 7 compares wind speed differences between the two systems. The periodic pattern is consistent with other data examined to date. The large differences near and above 3 km are on the high side, but values around ±1 m s^{-1} are not uncommon. Cogan (1995) presented data showing a few wind direction variations greater than 90° in one case during the LAFRE, although wind direction differences for most heights in the data examined to date were less than 10°. This type of comparison suggests that differences in profiler wind speed and direction of around ±1 m s^{-1} and 10°, respectively, relative to rawinsonde may be close to the "best" one could expect. A possible partial explanation for the wind speed differences is that the MARWIN software has more extensive built-in checks and somewhat smooths the data. Nevertheless, caution must be taken when using a rawinsonde sounding as a standard, especially in light winds. The user should make sure each sounding contains valid data and then apply appropriate quality controls.

b. Wallops Island

Field tests at the NASA Wallops Flight Facility (WFF) on Wallops Island, Virginia, provided the opportunity to compare MPS wind profiles for the lowest 1.9 km with wind profiles obtained from radar-tracked pibal balloons. An unusual aspect of this experiment as compared with other comparison studies such as the LAFRE and earlier work (e.g., Weber and Wuertz 1990) was the ability to examine the background wind variability at the same time as the comparisons. During the week of 17–21 July 1995, for morning and afternoon periods lasting about 1–1.5 h, two pibals were launched about 3 min apart every 15 min (four to five "pairs" each period). The MPS operated continuously during these periods producing wind profiles every 3 min. For each pibal pair, comparisons were made between the 3-min MPS profile just prior to the second pibal and the second pibal, and between the first and second pibal. Surface values shown were taken from the WFF and MPS surface sensors. The site of the experiment was about 0.2 km west of the ocean, with the MPS located less than 50 m east from the pibal launch site. Figures 8–11 show the means and standard deviations of the wind speed and direction differences between MPS and second pibal, and pibal pairs for 100-m layers on 20 July 1995 (nine "pairs") and 21 July 1995 (five "pairs").

The MPS versus pibal comparison for 18 July (not shown) showed significantly greater differences in wind direction than for the other two comparison days (20 and 21 July). The pibal versus pibal comparison for that day also showed somewhat larger differences in wind direction relative to those for the other days. The standard deviation of wind direction differences exceeded 10° for pibal versus pibal for heights $z \leq 0.3$ km and $z = 1.1$ km, and for the MPS versus pibal at $z \leq 0.8$ km and $z = 1.2$ km. The magnitude of mean differences in wind direction between MPS and pibal was greater or equal to 20° at $z = 0.6$ km, $0.8 \leq z \leq 1.2$ km, and $1.5 \leq z \leq 1.8$ km (maximum of about 25° at 1.6 km). Magnitude of mean and standard deviation of wind speed differences was somewhat larger at $z \leq 0.6$ km for the MPS versus pibal. Also, on this day the pibals traveled eastward, passing over the ocean within a minute after launch. These larger differences were therefore not unexpected since the pibals drifted over the ocean after reaching 200 or 300 m in altitude, leaving the highly convective conditions that existed over the land. Later in the afternoon small, but intense, thunderstorms passed through from the west, forcing the test to be canceled before 1500 EDT (1900 UTC) due to the danger of lightning strikes.

The largest direction difference between the MPS and pibal was at the "surface" (about 5 m AGL) for the latter two days and at 0.1 km on 18 July. Both systems relied on surface stations separated by about 10 m horizontally and 1–2 m vertically (the WFF anemometer
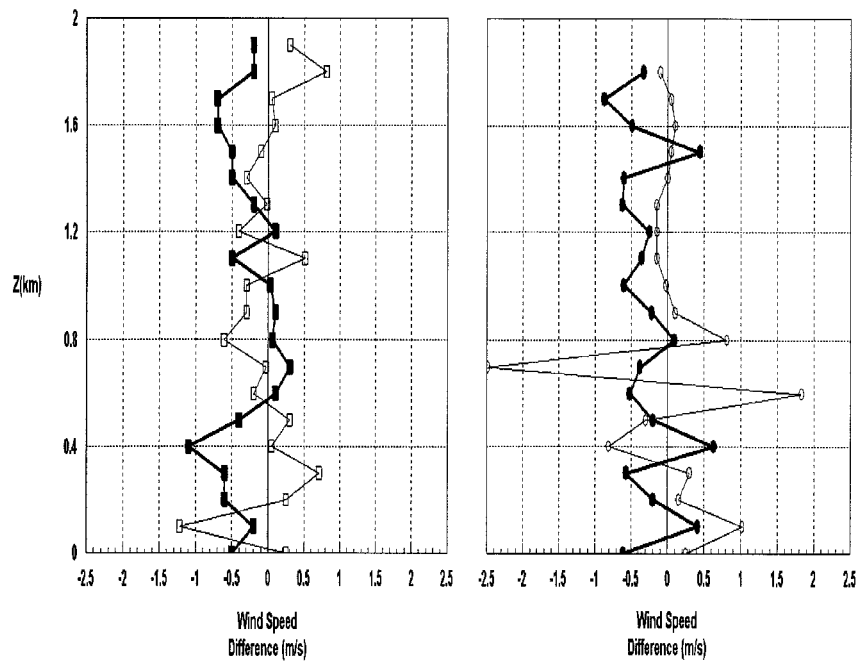
FIG. 8. Mean wind speed differences (m s^{-1}) from WFF data. Bold curves represent MPS versus pibal, lighter ones represent pibal versus pibal. Left graph (square data points) and right graph (circles) are plots for 20 and 21 July, respectively. Heights are AGL.

was higher). The location, only about 200 m from the ocean, and the mix of land and water surfaces near the launch site, may account for much of the observed direction differences in the lowest 0.1–0.2 km. The balloons drifted off roughly to the northwest except on 18 July, soon after turning toward the east to northeast,

passing over the northern half of the island, and out over the water. Since the ascent rate of the pibals was about 5 m s^{-1} and the average wind speed for most of the test periods was about 5–7 m s^{-1} during much of each ascent, the balloon ended up about 2–3 km from the MPS and pibal launch site by the time it reached
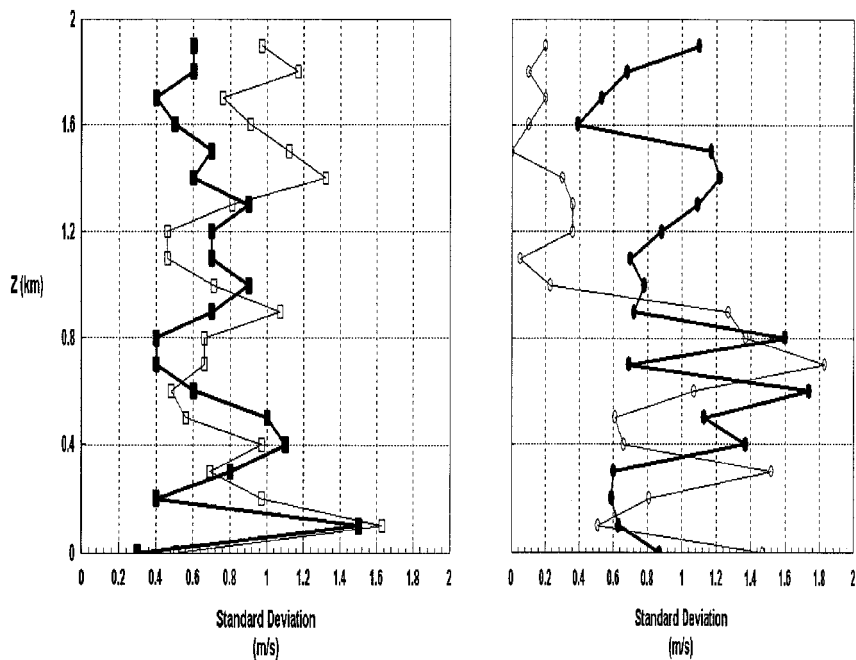

FIG. 9. As in Fig. 8 except plotted for standard deviation of wind speed differences (m s^{-1}).
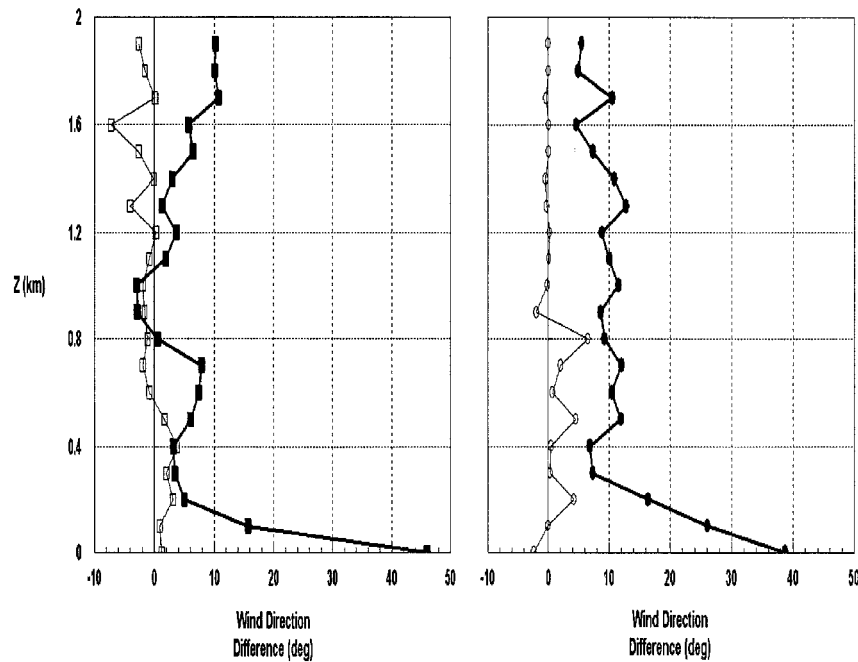
FIG. 10. As in Fig. 8 except plotted for mean wind direction differences (deg).

an altitude of 2 km. On 21 July the wind speed at most heights exceeded 10 m s^{-1}, causing the pibal to drift about 4 km by the time it rose to 2 km.

The comparison of wind profiling radar with radar-tracked pibals yielded results for wind speed that appear better than those shown in Table 3. The average magnitude of mean differences (0.1-km layers) from the WFF data (Fig. 8) appears similar to that from the LAF-RE data for 7–11 September 1993. However, the average of the means from the LAFRE for 17–23 September is considerably larger. The standard deviations of the differences for all layers in Fig. 9 are less than the average standard deviation of either period in Table 3. The average standard deviation between MPS and pibal in Fig. 9 is about 0.8 m s^{-1}. The accuracies suggested using data from the WFF experiment (Figs. 8–11) appear better overall than those presented in Table 2 for radar profilers, except for the wind direction on 18 July. The differences between values in Figs. 8–11 and Tables 2 and 3, and variations between profiles from pibals launched 3 min apart (also Figs. 8–11), support the idea that differences between radar profiler and rawinsonde wind soundings in earlier LAFRE data indeed may be at least partly a result of real atmospheric temporal and spatial variation. The data for 18 July, with even larger standard deviations of wind direction differences for both pibal versus pibal and MPS versus pibal than those for 20 and 21 July, suggest that these variations can be significant even over a 3-min time span.

The Wallops Island experiment provided an opportunity to test a new type of surface-based radiometer, which was developed for ARL by the OPHIR Corporation. This new radiometer, the Next Generation Ra-diometer (NGR), incorporates several design advances over the older system [the Passive Microwave Temperature Profiler (PMTP)], including a much smaller size and lighter weight and, notably, frequency tunability and very precise software control of radiometer frequency in the oxygen bands. The antenna system for the NGR is based on an optical lens that focuses into a corrugated horn antenna.

The PMTP uses Gunn diodes for local oscillators for all measurements. There are four such oscillators limiting measurement to four frequencies. The oscillators also suffer from a tendency to drift in frequency when their temperatures are not precisely controlled and require frequent calibration to check for drift due to mechanical effects. In the NGR, the oxygen band local oscillator is a highly stable tunable synthesizer. This frequency tunability of NGR makes it practical to use a larger number of frequencies (for this experiment, 11 frequencies) in the 50–60-GHz sensing band. The PMPT is restricted to four frequencies.

In the Wallops experiment, the performance of the radiometers, as measured by comparison with simultaneous radiosonde observations, was comparable at lower levels, but the NGR appeared definitely superior at the higher levels. Figure 12 shows root-mean-square differences for nine comparisons between simultaneous radiosonde observations and corresponding measurements with the current ARL oxygen radiometer system (PMTP) and the OPHIR radiometer (NGR).

5. Conclusions

The Mobile Profiling System (MPS) shows promise as a means of collecting data from a variety of profiling
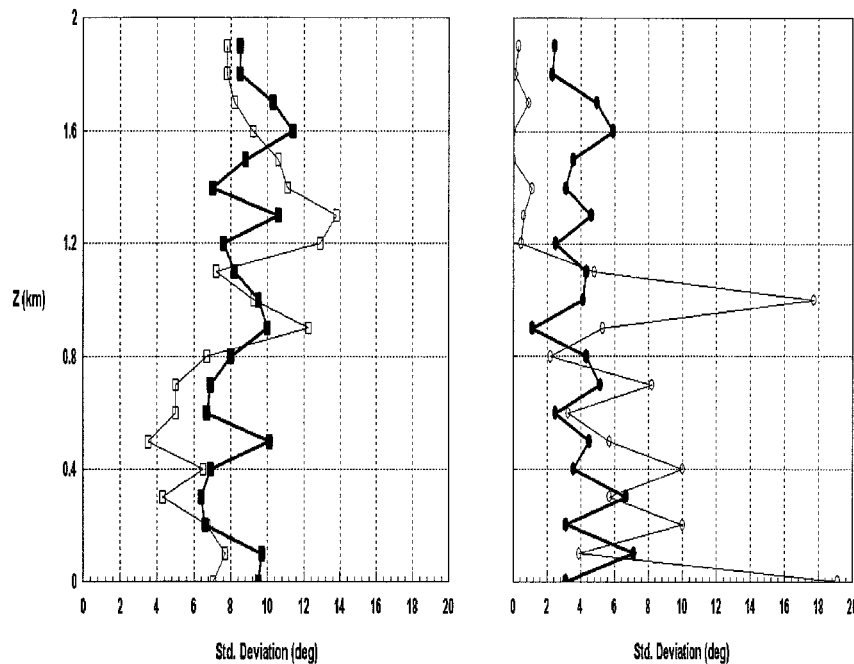
FIG. 11. As in Fig. 8 except plotted for standard deviation of wind direction differences (deg).

instruments and merging these data into combined meteorological soundings for near-real-time operational applications. The merging method provides soundings with an accuracy in temperature (or virtual temperature) comparable to rawinsonde soundings or to other currently published methods of combining ground-based and satellite data. While the MW radiometer component of the MPS uses a priori information, the merging algorithm has the advantage of not being site specific and a priori datasets are not required as in statistical merging techniques. It also may be used to combine profiles of other meteorological variables. However, the accuracy of wind velocity values above the maximum radar data level is limited by the errors in current methods of deriving wind velocity from satellite sounder data. New ways to derive satellite wind velocities are being investigated. In the interim, merging wind data from conventional systems (e.g., rawinsondes) for the upper part of the sounding may be the only viable alternative. The combining algorithm is not limited to the MPS. It also can be applied to other suites of instruments capable of measuring profiles. Existing facilities where this algorithm may prove useful include the NOAA NPN and systems at sites within or near airports and at government test ranges. The basic method may be applied to airborne systems as well.
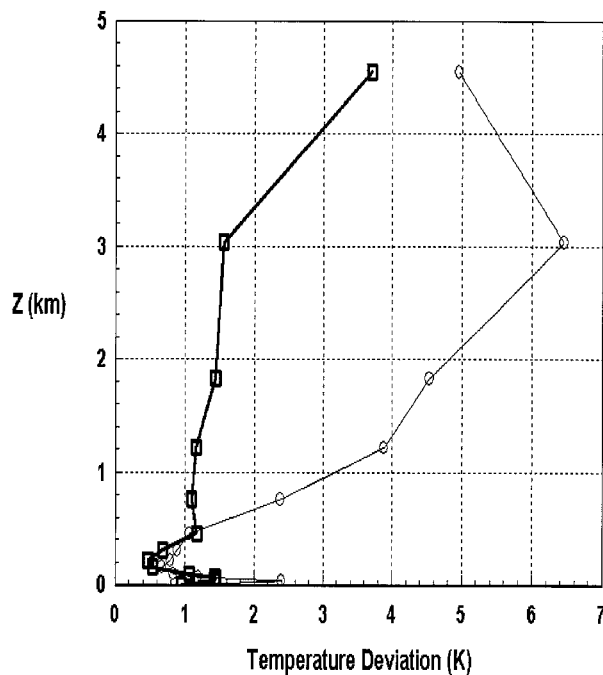
The data provided by the MPS will have a variety of civilian and military applications. The MPS can provide timely support for airfield operations, giving, for example, near-real-time indications of potentially hazardous wind conditions. As the Los Angeles Free Radical Experiment showed, this type of system can be invaluable for pollution studies. The ability to generate a picture of very short-term flow and virtual temperature patterns in the lower troposphere can lead to a better understanding of the atmosphere and to better modeling at smaller scales.

FIG. 12. The rms deviations from NGR (bold squares) and PMPT (lighter circles) from concurrent rawinsonde observations.

Acknowledgments. The authors wish to acknowledge Florence Patten and Judy Kilmon of WFF, NASA, through whose efforts we obtained the pibal data at Wallops Island, and John Cruncleton and Richard Okrasinski, who provided key assistance in the computer drawing of Figs. 3–12.

REFERENCES

Barth, M. F., R. B. Chadwick, and D. W. van de Kamp, 1994: Data processing algorithms used by NOAA's wind profiler demostration network. *Ann. Geophys.,* **12,** 518–528.

Cogan, J., 1995: Test results from a Mobile Profiler System. *Meteor. Appl.,* **2,** 97–107.

——, and A. Izaguirre, 1993: A preliminary method for atmospheric soundings in near real time using satellite and ground-based remotely sensed data. U.S. Army Research Laboratory ARL-TR-240, DTIC Acquisition No. ADA274381, 45 pp. [Available on-line from http://www.dtic.dla.mil.]

Fisher, E. E., F. Brousaides, E. Keppel, F. J. Schmidlin, H. C. Herring, and D. Tolzene, 1987: Meteorological data error estimates. Meteorology Group, Range Commanders Council Document 353-87, 23 pp. [Available from U.S. Army Research Laboratory, AMSRL-IS-EA, White Sands Missile Range, NM 88002-5501.]

Flowers, W., L. Parker, G. Hoidale, E. Santonin, and J. Hines, 1994: Evaluation of a 924 MHz wind profiling radar. U.S. Army Research Laboratory ARL-CR-101, DTIC Acquisition No. ADA283782, 195 pp. [Available from U.S. Army Research Laboratory, White Sands Missile Range, NM 88002-5501.]

Franklin, J. L., and S. J. Lord, 1988: Comparisons of VAS and omega dropwindsonde thermodynamic data in the environment of Hurricane Debby (1982). *Mon. Wea. Rev.,* **116,** 1690–1701.

Heacock, L. E., Ed., 1985: Comparison of the Defense Meteorological Satellite Program (DMSP) and the NOAA Polar-Orbiting Operational Environmental Satellite (POES) program. Envirosat-2000 Rep., DTIC Acquisition No. ADA165118, National Oceanic and Atmospheric Administration, National Environmental Satellite, Data, and Information Service, 426 pp. [Available on-line from http://www.dtic.dla.mil.]

Jedlovec, G. J., 1985: An evaluation and comparison of vertical profile data from the VISSR Atmospheric Sounder (VAS). *J. Atmos. Oceanic Technol.,* **2,** 559–581.

Le Marshall, J. F., 1988: An intercomparison of temperature and moisture fields derived from TIROS operational vertical sounder data by different retrieval techniques. Part I: Basic statistics. *J. Appl. Meteor.,* **27,** 1282–1293.

May, P. T., K. P. Moran, and R. G. Strauch, 1989: The accuracy of RASS temperature measurements. *J. Appl. Meteor.,* **28,** 1329–1335.

Merritt, D., 1995: A statistical averaging method for wind profile Doppler spectra. *J. Atmos. Oceanic Technol.,* **12,** 985–995.

Moran, K. P., and R. G. Strauch, 1994: The accuracy of RASS temperature measurements corrected for vertical air motion. *J. Atmos. Oceanic Technol.,* **11,** 995–1001.

Okrasinski, R. J., and R. O. Olsen, 1991: Intercomparison of wind measurements from two Doppler SODARS, a UHF profiling radar, rawinsondes, and in situ tower sensors. Preprints, *Symp. on Lower Tropospheric Profiling: Needs and Technologies,* Boulder, CO, Amer. Meteor. Soc., 121–122.

Orlanski, I., 1975: A rational subdivision of scales for atmospheric processes. *Bull. Amer. Meteor. Soc.,* **56,** 527–530.

Parsons, D., and Coauthors, 1994: The integrated sounding system: Description and preliminary observations from TOGA COARE. *Bull. Amer. Meteor. Soc.,* **75,** 553–567.

Ralph, R. M., P. J. Neiman, D. W. van de Kamp, and D. C. Law, 1995: Using spectral moment data from NOAA's 404-MHz radar wind profilers to observe precipitation. *Bull. Amer. Meteor. Soc.,* **76,** 1717–1739.

Reale, A. L., 1990: Baseline upper air network (BAUN) final report. NOAA Tech. Rep. NESDIS 52, DTIC Acquisition No. ADA 229638, 57 pp. [Available on-line from http://www.dtic.dla.mil.]

Schroeder, J. A., E. R. Westwater, P. T. May, and L. M. McMillin, 1991: Prospects for temperature sounding with satellite and ground-based RASS measurements. *J. Atmos. Oceanic Technol.,* **8,** 506–513.

Shenk, W. E., T. H. Vonder Haar, and W. L. Smith, 1987: An evaluation of observations from satellites for the study and prediction of mesoscale events and cyclone events. *Bull. Amer. Meteor. Soc.,* **68,** 21–35.

Stokes, G. M., and S. E. Schwartz, 1994: The Atmospheric Radiation Measurement (ARM) Program: Programmatic background and design of the cloud and radiation test bed. *Bull. Amer. Meteor. Soc.,* **75,** 1201–1221.

Strauch, R. G., D. A. Merritt, K. P. Moran, K. B. Earnshaw, and D. C. Welsh, 1984: The Colorado wind profiling network. *J. Atmos. Oceanic Technol.,* **1,** 37–49.

Swadley, S. D., and J. Chandler, 1992: The defense meteorological satellite program's special sensor microwave imager/sounder (SSMIS): Hardware and retrieval algorithms. Preprints, *Sixth Conf. on Satellite Meteorology and Oceanography,* Atlanta, GA, Amer. Meteor. Soc., 457–461.

Weber, B. L., and D. B. Wuertz, 1990: Comparison of rawinsonde and wind profiler radar measurements. *J. Atmos. Oceanic Technol.,* **7,** 157–174.

——, and Coauthors, 1990: Preliminary evaluation of the first NOAA demonstration network wind profiler. *J. Atmos. Oceanic Technol.,* **7,** 909–918.

Westwater, E. R., W. B. Sweezy, L. M. McMillin, and C. Dean, 1984a: Determination of atmospheric temperature from a statistical combination of ground-based profiler and operational NOAA 6/7 satellite retrievals. *J. Climate Appl. Meteor.,* **23,** 689–703.

——, W. Zhendui, N. C. Grody, and L. M. McMillin, 1984b: Remote sensing of temperature profiles by a combination of ground-based profiler and satellite-based MSU radiometric observations, Preprints, *Conf. on Satellite/Remote Sensing and Applications,* Clearwater, FL, Amer. Meteor. Soc., 191–196.

Wilczak, J. M., and Coauthors, 1995: Contamination of wind profiler data by migrating birds: Characteristics of corrupted data and potential solutions. *J. Atmos. Oceanic Technol.,* **12,** 449–467.

Wolfe, D., and Coauthors, 1995: An overview of the mobile profiler system: Preliminary results from field tests during the Los Angeles free-radical study. *Bull. Amer. Meteor. Soc.,* **76,** 523–534.